Biophysical *Journal*
Article

Biophysical Society

Intracellular Requirements for Passive Proton Transport through the Na^+,K^+-ATPase

Kevin S. Stanley,[1,2] Dylan J. Meyer,[2] Craig Gatto,[1] and Pablo Artigas[2,*]
[1]Department of Biological Sciences, Illinois State University, Normal, Illinois; and [2]Department of Cell Physiology and Molecular Biophysics, Center for Membrane Protein Research, Texas Tech University Health Sciences Center, Lubbock, Texas

ABSTRACT The Na^+,K^+-ATPase (NKA or Na/K pump) hydrolyzes one ATP to exchange three intracellular Na+ (Na^+_i) for two extracellular K+ (K^+_o) across the plasma membrane by cycling through a set of reversible transitions between phosphorylated and dephosphorylated conformations, alternately opening ion-binding sites externally (E2) or internally (E1). With subsaturating $[Na^+]_o$ and $[K^+]_o$, the phosphorylated E2P conformation passively imports protons generating an inward current (I_H), which may be exacerbated in NKA-subunit mutations associated with human disease. To elucidate the mechanisms of I_H, we studied the effects of intracellular ligands (transported ions, nucleotides, and beryllium fluoride) on I_H and, for comparison, on transient currents measured at normal Na^+_o (Q_{Na}). Utilizing inside-out patches from *Xenopus* oocytes heterologously expressing NKA, we observed that 1) in the presence of Na^+_i, I_H and Q_{Na} were both activated by ATP, but not ADP; 2) the $[Na^+]_i$ dependence of I_H in saturating ATP showed $K_{0.5,Na} = 1.8 \pm 0.2$ mM and the [ATP] dependence at saturating $[Na^+]_i$ yielded $K_{0.5,ATP} = 48 \pm 11$ μM (in comparison, Na^+_i-dependent Q_{Na} yields $K_{0.5,Na} = 0.8 \pm 0.2$ mM and $K_{0.5,ATP} = 0.43 \pm 0.03$ μM; 3) ATP activated I_H in the presence of K^+_i (~15% of the I_H observed in Na^+_i) only when Mg^{2+}_i was also present; and 4) beryllium fluoride induced maximal I_H even in the absence of nucleotide. These data indicate that I_H occurs when NKA is in an externally open E2P state with nucleotide bound, a conformation that can be reached through forward Na/K pump phosphorylation of E1, with Na^+_i and ATP, or by backward binding of K^+_i to E1, which drives the pump to the occluded E2(2K), where free P_i (at the micromolar levels found in millimolar ATP solutions) promotes external release of occluded K^+ by backdoor NKA phosphorylation. Maximal I_H through beryllium-fluorinated NKA indicates that this complex mimics ATP-bound E2P states.

INTRODUCTION

Maintaining Na^+ and K^+ in electrochemical disequilibrium between the cytoplasm and extracellular milieu is critical for the physiology of animal cells, as the potential energy stored in these electrochemical gradients is exploited for common cellular processes such as cell volume regulation, pH balance, excitability, and secondary active transport. These gradients are established and maintained solely by the Na^+,K^+-ATPase (NKA, also known as the Na/K pump), a member of the P-type ATPase family of integral membrane proteins, which primarily use the chemical energy in ATP to transport ions across the lipid bilayer against their electrochemical gradients.

In each catalytic cycle, the NKA transports three Na^+ ions out of the cell in exchange for two K^+ ions at the cost of one ATP molecule (1) while transiting through the cycle of fully reversible partial reactions known as the Post-Albers kinetic scheme (Fig. 1), alternating between the phosphorylated and dephosphorylated forms of two major conformations: E1, in which the ion-binding sites open to the inside, and E2, where the ion-binding sites open to the outside (2). The forward cycle (clockwise in Fig. 1) starts when three Na^+_i ions bind to the intracellularly facing sites, promoting phosphorylation of the pump from ATP (with high affinity, $K_{0.5} < 1$ μM) and forming E1P with the concomitant occlusion of three Na^+ ions within the protein. E1P spontaneously relaxes to E2P, leading to external Na^+ release. Subsequent binding of two K^+_o closes external ion access as the 2 K^+ ions are occluded, accelerating hydrolysis of the phosphoenzyme and P_i release. The rate-limiting step in the cycle is K^+ deocclusion and release to the inside by the dephosphorylated pump, a reaction that is significantly accelerated by direct binding of ATP with low affinity ($K_{0.5}$ ~100 μM, without hydrolysis).

In addition to the full reaction cycle, which produces an outward current due to extrusion of one net charge per cycle (3), several other Na/K pump partial reactions produce

Submitted July 14, 2016, and accepted for publication September 28, 2016.
*Correspondence: pablo.artigas@ttuhsc.edu
Kevin S. Stanley and Dylan J. Meyer contributed equally to this work.
Editor: Ian Forster.
http://dx.doi.org/10.1016/j.bpj.2016.09.042

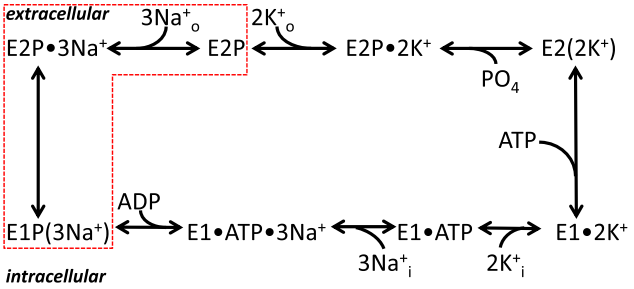

FIGURE 1 Post-Albers reaction scheme of NKA function. The dotted box shows the transitions responsible for voltage-dependent transient charge movement. To see this figure in color, go online.

electrical signals. When voltage pulses are applied in the absence of K^+_o and the presence of Na^+_o with Na^+_i and ATP, the voltage-dependent release and rebinding of Na^+ from the external side produce a transient current, also known as the transient charge movement (Q_{Na}), as the protein transitions between the Na-occluded E1P($3Na^+$) and Na^+-free E2P states (4,5). A similar external binding reaction, with lower voltage dependence, is seen in the absence of Na^+_o, with nonsaturating K^+_o and K^+_i and P_i (6,7), although measurement of this reaction requires large membrane surfaces with a very high Na/K pump density.

Another current-producing functional mode occurs in the absence of externally saturating $[Na^+]_o$ and $[K^+]_o$ (i.e., when externally facing sites are not fully occupied). In this instance, the passive permeation of protons by the NKA generates a voltage-dependent inward current (I_H) at negative potentials. Over the last 20 years, many laboratories have characterized I_H, focusing mainly on its extracellular requirements and the effect of mutagenesis (8–16), which led to the current view suggesting that protons are imported when the pump is in E2P. However, studies of the intracellular requirements for this current have been limited (17).

The NKA is composed of a catalytic α-subunit (of which there are four isoforms) and an auxiliary β-subunit (with three isoforms). Aside from I_H through wild-type Na/K pumps, some disease-related mutations of the α1 and α2 subunits also modify its transport characteristics and induce passive currents (sometimes referred to as leak currents) under conditions with high Na^+_o (where wild-type I_H is negligible due to near saturation of externally facing sites with Na^+ and K^+). All hyperaldosteronism-inducing α1 mutations studied so far (18), as well as one mutation in the α2 subunit linked to familial hemiplegic migraine (13,19), display inward currents at negative voltages (see also (20) for a recent review). These modified leak currents, some of which appear to transport Na^+ instead of H^+, were proposed to be a gain-of-function that mediates the pathophysiological effect of the mutations (18).

Here, we used giant patches excised from *Xenopus* oocytes heterologously expressing ouabain-resistant pumps to perform a detailed study of the intracellular requirements for I_H in the absence of Na^+_o, and compared them with the requirements for Q_{Na} in the presence of Na^+_o. Although our results reveal that both transport modes require phosphorylated pumps, we observed a large distinction between these two transport modes: in the presence of Na^+_i, maximal I_H requires low-affinity binding of ATP to E2P ($K_{0.5}$ ~100 μM), whereas Q_{Na} only requires phosphorylation by ATP with high affinity ($K_{0.5}$ ~0.5 μM). Finally, we demonstrate that beryllium-fluorinated (i.e., NKA-BeF_3^-) pumps present I_H even in the absence of nucleotide, suggesting that the conformation promoted by this phosphate analog mimics an externally open E2P state with nucleotide bound to the pump. These results are discussed in the context of the Post-Albers scheme (Fig. 1) and previous studies of partial reactions of the Na/K pump.

MATERIALS AND METHODS

Oocyte preparation and molecular biology

Oocytes were enzymatically isolated by 1–2 h of incubation (depending on the degree of desired defolliculation) in Ca^{2+}-free OR2 solution at pH 7.4 (in mM: 82.5 NaCl, 2 KCl, 1 $MgCl_2$, 5 HEPES) with 0.5 mg/mL collagenase type IA. Enzymatic treatment was followed by four 15-min rinses in Ca^{2+}-free OR2 and two rinses in OR2 with 1.8 mM Ca^{2+}. The ouabain-resistant *Xenopus* Q120R/N131D (RD)-α1 and the β3 subunit, both in the pSD5 vector, were linearized with *Bgl*II and transcribed with an SP6 mMESSAGE mMACHINE (Thermo Fisher Scientific, Waltham, MA). Oocytes were injected with an equimolar mixture of cRNA for RD-α1 and β3 cRNA, and then maintained in SOS solution (in mM: 100 NaCl, 2 KCl, 1.8 $CaCl_2$, 1 $MgCl_2$, and 5 HEPES) supplemented with horse serum and antimycotic-antibiotic solution (Gibco Anti-Anti; Thermo Fisher Scientific) at 16°C for 2–6 days until recordings were obtained. The RD double substitution mimics the residues responsible for the naturally ouabain-resistant rat-α1 subunit (21), allowing for selective inhibition of endogenous pumps with 1 μM ouabain and the acquisition of measurements exclusively from exogenous pumps.

Solutions

Extracellular solutions contained 1 μM ouabain and (in mM) 133 methane sulfonic acid, 10 HEPES, 5 $Ba(OH)_2$, 1 $Mg(OH)_2$, 0.5 $Ca(OH)_2$, titrated to pH 6.0 with 125 N-methyl D-glucamine (NMG^+) or to pH 7.6 with NaOH. Cl^- (10 mM) was added to pipette solutions by mixing with 125 mM NMG-Cl or NaCl to maintain electrode reversibility. The cytoplasmic bath solution for patch experiments contained (in mM) 110 glutamic acid, 10 tetraethylammonium-Cl, 10 HEPES, 5 EGTA, 1 $MgCl_2$, pH 7.4, with 110 NMG, KOH, or NaOH. Intermediate Na^+_i and K^+_i concentrations were obtained by mixing Na^+_i or K^+_i with NMG^+_i. The osmolality of all recording solutions was 250–260 mOsmol/kg. MgATP, $TRIS_2ATP$, Na_2ADP, KADP, or K_2HPO_4 was added from 200 mM stocks (pH 7.4 with NMG^+_i). Adenosine 5′-(β,γ-imido)triphosphate (AMPPNP, tetra Li^+ salt) was directly added to the solutions (brought to pH 7.4 with NMG^+). All nucleotides were obtained from Sigma-Aldrich (St. Louis, MO). Equimolar Mg^{2+} was added from a 200 mM $MgCl_2$ stock to all intracellular solutions to which Li^+, K^+, or Na^+ nucleotide salt was added to maintain ~1 mM free Mg^{2+} (except for the experiment shown in Fig. 8, where Mg^{2+} was omitted from the intracellular solution). Beryllium fluoride was added from a stock solution containing 10 mM $BeSO_4$ and 250 mM NaF (pH 7.4 with NMG^+) to form the NKA-BeF_3^- complex.

Electrophysiology

Giant patches were formed and excised 3–6 days after oocyte injection using fire-polished, wide-tipped (~20 μm diameter), thick-walled borosilicate pipettes coated with Sylgard. The extracellular pipette solution was either NMG^+_o at pH 6.0 (to measure I_H) or Na^+_o at pH 7.6 (to measure Q_{Na}) with 1 μM ouabain to inhibit endogenous Na/K pumps. A Dagan 3900A integrating patch-clamp amplifier, Digidata 1322 or 1550A A/D board, and pClamp software (Molecular Devices, Sunnyvale, CA) were used for data acquisition at 20 or 100 kHz (filtered at 5 or 10 kHz).

Determination of P_i in ATP solutions

To determine free P_i, we employed the same ammonium molybdate colorimetric assay used in our previous Na^+,K^+-ATPase assays (22,23). Briefly, we generated a standard curve by diluting a 1 mM Na_2PO_4 solution into duplicate samples of 1, 5, 10, 20, 50, and 100 μM final [Na_2PO_4] in a 0.5 mL total volume of NMG intracellular solution. Similarly, 0.5 mL of the same intracellular solution containing 4 mM of MgATP was prepared in duplicate. The vials were incubated at room temperature for 60 min and 1 mL of stopping solution (330 mM ascorbic acid, 0.5% ammonium molybdate, 0.5 M HCl) was added and further incubated for 10 min at room temperature. Then 1.5 mL of ACG solution (20 g/L Na-arsenate, 20 g/L Na-citrate, and 2% glacial acetic acid) was added and incubated for 5 min at room temperature, and sample absorbance was determined at 800 nm (VersaMax microplate reader; Molecular Devices). The amount of P_i present in the ATP solutions was determined by the slope of the standard curve.

Data analysis

Nucleotide and Na^+_i apparent affinities ($K_{0.5}$) were obtained by fitting the data to the Hill equation:

$$\begin{aligned} I &= I_{max}([S]^{n_H}/(K_{0.5}^{n_H} + [S]^{n_H})) \text{for inward current} \\ &\text{or} \\ Q_{tot} &= Q_{max}([S]^{n_H}/(K_{0.5}^{n_H} + [S]^{n_H})) \text{for transient} \\ &\text{charge movement.} \end{aligned} \quad (1)$$

A rectangular hyperbola was used for nucleotides (Eq. 1, $n_H = 1$).

Transient charge (Q) movement was obtained by integrating the area under the relaxation curve in the OFF (as in Ref. (24)). Charge versus voltage (Q-V) curves were fitted with a Boltzmann distribution:

$$Q = Q_{hyp}\text{-}Q_{tot}/\left(1 + \exp\left(z_q e\left(V\text{-}V_{1/2}\right)/kT\right)\right), \quad (2)$$

where Q_{hyp} is the charge moved by hyperpolarizing voltage pulse, Q_{tot} is the total charge moved, $V_{1/2}$ is the center of the distribution, z_q is the apparent valence of an equivalent charge that traverses the whole membrane electric field, and e, k, and T have their usual meanings (cf. Ref. (25)). kT/e = 25.4 mV at room temperature (22°C in our experiments); kT/ez_q is also called the slope factor because it refers to the steepness of the curve.

All analyses were performed using pClamp and Origin (OriginLab, Northampton, MA). All intracellular $K_{0.5}$ values were obtained at pH 7.4.

RESULTS

Activation of I_H by Na^+_i

A typical experiment from an inside-out patch exposed to a pH 6 NMG^+ extracellular solution in the pipette demonstrates that MgATP activates I_H when added to a solution containing 20 mM Na^+_i, but not when NMG^+_i is the only intracellular monovalent cation (Fig. 2). The holding current ($V_h = -50$ mV) recorded using a slow time base exhibits ramp-shaped vertical deflections in the continuous trace corresponding to the application of 50-ms-long step voltage pulses. The currents induced by such pulses at the times indicated by lowercase letters in Fig. 2 *A* are shown at a faster acquisition rate (20 kHz, filter 5 kHz) in Fig. 2 *B*. The current-voltage (I-V) curves (Fig. 2 *C*) plot the average steady-state current of the MgATP-induced signal (current with MgATP minus current without MgATP; i.e., b − a and d − c) during the last 5 ms of the pulses against the applied voltage. Activation of I_H by Na^+_i and MgATP resembles the requirements for activation of transient currents in the presence of external Na^+ (Q_{Na}) when inside-out patches are bathed by Na^+_i and MgATP (24,26).

We measured the Na^+_i concentration dependence of I_H in the presence of 4 mM MgATP (Fig. 3). Stepwise increases in $[Na^+]_i$ on a typical patch held at −80 mV gradually increased the inward holding current, an effect that was reversed by MgATP withdrawal (Fig. 3 *A*). The normalized I_H-V plots at different $[Na^+]_i$ values (Fig. 3 *B*) illustrate their similar voltage dependences. The average MgATP-activated current at −140 mV was plotted as a function of $[Na^+]_i$ (Fig. 3 *C*) and fitted to Eq. 1 (*solid line*) to obtain the apparent Na^+ affinity (inverse of $K_{0.5}$). The best fit parameters, $K_{0.5} = 1.8 \pm 0.2$ mM and $n_H = 1.7 \pm 0.2$, are similar to those previously reported for Na^+_i activation of Q_{Na} (*dotted line*, $K_{0.5} = 0.8 \pm 0.1$ mM; $n_H = 2.5 \pm 0.6$, $n = 5$ (24)).

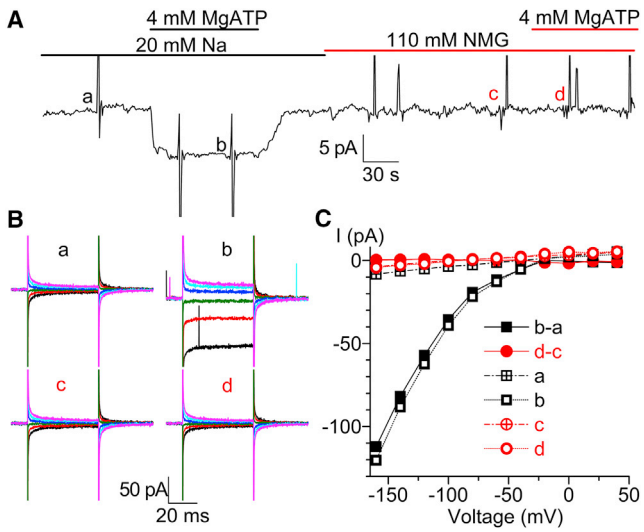

FIGURE 2 I_H activation by Na^+_i and ATP. (*A*) Continuous current recording from a patch held at −50 mV, 4 days after cRNA injection. (*B*) Fast temporal resolution of the family of current traces obtained at the times indicated by small caps (a–d) in (*A*) by pulses to −160 mV, −120 mV, −80 mV, −40 mV, 0 mV, and +40 mV. (*C*) I-V plot of the average current during the last 5 ms of each pulse, as a function of the applied voltage in a–d and the MgATP-activated current (a-b and c-d). To see this figure in color, go online.

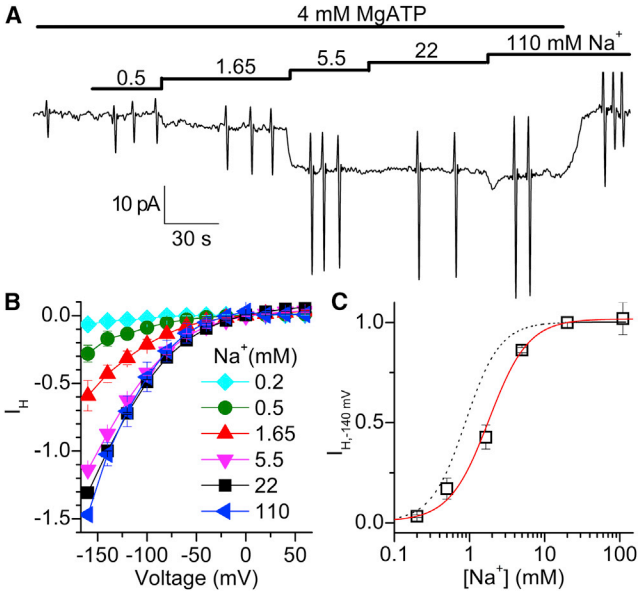

FIGURE 3 Na^+_i dependence of I_H. (*A*) Recording from a patch at $V_h = -80$ mV in the presence of different $[Na^+_i]$. (*B*) MgATP-activated I-V curves at the indicated $[Na^+_i]$, normalized to I_H at −140 mV, 20 mM Na^+_i. (*C*) I_H at −140 mV as a function of $[Na^+_i]$. The solid line represents a fit to the Hill function (Eq. 1), with parameters in the text. The dotted line represents a fit of the $[Na^+_i]$-dependence of charge movement to Eq. 1 (from Ref. (24)). Data in (*B*) and (*C*) are means ± SEM from four patches. To see this figure in color, go online.

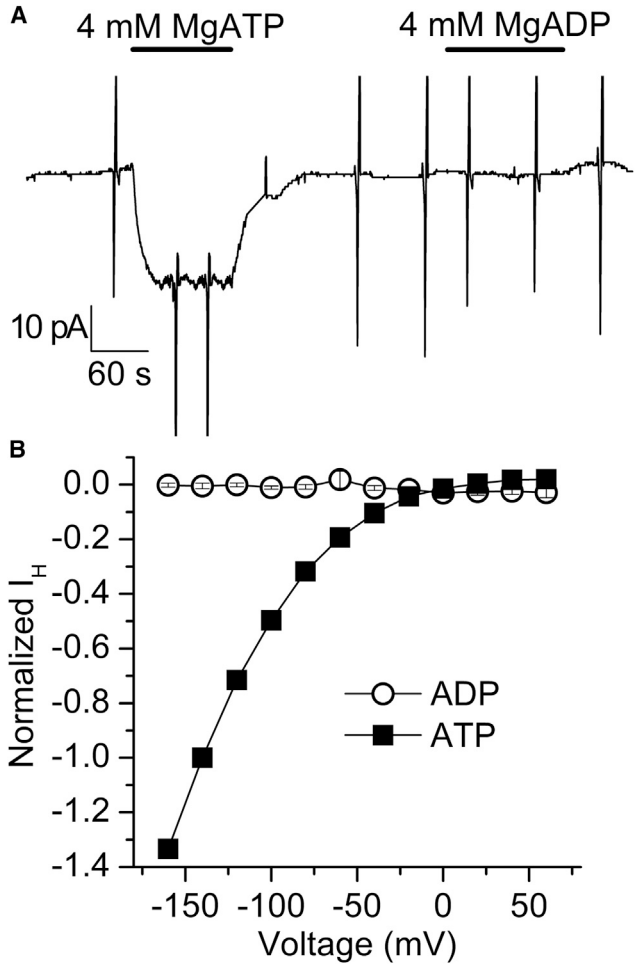

FIGURE 4 Nucleotide effects on I_H with 20 mM Na^+_i. (*A*) Recording from a patch at $V_h = -50$ mV on which MgATP and MgADP (4 mM) were applied. (*B*) Nucleotide-induced I_H-V curve normalized to the I_H at −140 mV with MgATP. Data are means ± SEM from six patches.

Nucleotide dependences of I_H and Q_{Na} in Na^+_i solutions

The apparent affinity for activation of I_H by Na^+_i is ~10-fold higher than the apparent affinity of processes with significant cycling, such as Na^+,K^+-ATPase activity ($K_{0.5}$ = 10–20 mM (27,28)), where the fractional occupancy of the E1 state that binds Na^+_i is reduced. Given that Na^+_i and MgATP facilitate I_H, we hypothesized that phosphorylation is required to activate I_H. We tested this directly by determining the effect of adding ADP (Fig. 4, *A* and *B*) or nonhydrolysable ATP analogs that are known to interact with the pump (29,30) (i.e., AMPPNP (cf. Fig. 7 below) and AMPPCP (not shown)). As expected, sole application of these nucleotides did not activate I_H, demonstrating that phosphorylation is required for I_H to occur in the presence of Na^+_i.

Phosphorylation by ATP of the E1 conformation in the presence of Na^+_i occurs with high apparent affinity ($K_{0.5ATP} < 1$ μM) (31). In contrast, there is a low-affinity interaction of ATP with E2 states, which is known to accelerate K^+ deocclusion in the normal cycle ($K_{0.5ATP}$ ~100 μM) (31). To obtain a more complete picture of the states required for each noncanonical current mode, we compared the ATP concentration dependences of Q_{Na} (Fig. 5) and I_H (Fig. 6), which have not been reported previously. The superimposed current traces from a patch bathed in 125 mM Na^+_o (Fig. 5 *A*) were obtained by subtracting the current elicited by pulses from −50 mV to −160 mV and +40 mV in the absence of ATP from current induced by the same pulses with 1 μM ATP (*thick line*) or 4 mM ATP (*thin line*). The integrals of the ATP-induced transient currents when the pulses were returned to −50 mV (Q_{OFF}) in the same patch were plotted against the pulse voltage in the Q_{OFF}-V plot (Fig. 5 *B*). The normalized Q_{tot}, obtained from the Boltzmann fits of the Q-V curves at different [ATP] values (Fig. 5 *C*) were plotted as a function of [ATP] (Fig. 5 *D*). The $K_{0.5ATP}$ = 0.43 ± 0.03 μM shows that Q_{Na} requires only phosphorylation of the pumps, and not low-affinity binding of ATP to E2. Also, ATP binding does not significantly alter the Q-V curve position on the voltage axis, as there is no correlation between [ATP] and the similar $V_{1/2}$ values (one-way ANOVA, $p = 0.32$; SAS software, SAS Institute, Cary, NC).

A different response was observed from the [ATP] dependence of I_H (Fig. 6). A representative recording obtained at −80 mV from a patch with NMG^+_o (pH 6.0) solution in the pipette illustrates a full-dose response for ATP in 20 mM

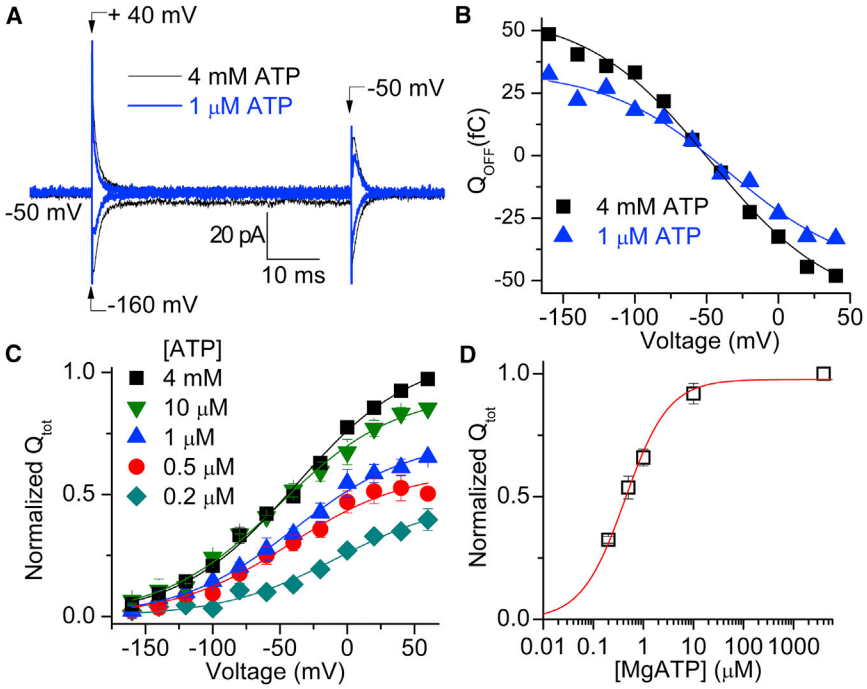

FIGURE 5 MgATP activation of Q_{Na} in 20 mM Na^+_i, with 125 mM Na^+_o (pH 7.6). (*A*) MgATP-induced current (current in ATP minus current without ATP) elicited by voltage pulses from V_h = −50 mV to −160 mV or +40 mV. (*B*) Q_{OFF}-V curve for the patch in (*A*). Continuous lines represent global fits using the Boltzmann function (Eq. 2) with a shared slope factor kT/ez_q = 43 mV, Q_{tot} = 81.3 fC, $V_{1/2}$= −35 mV at 1 μM MgATP, and Q_{tot} = 120 fC, $V_{1/2}$ = −41 mV at 4 mM MgATP. (*C*) Average Q_{OFF}-V curves from five patches in which different [MgATP] were applied, normalized to Q_{tot} at 4 mM MgATP. Lines represent fits of Eq. 2 to the average data; the best fit $V_{1/2}$ values were −7.2 ± 9.0, −42 ± 4.7, −38 ± 5.2, −50 ± 5.2, and −38 ± 4.5 mV for 0.2 μM, 0.5 μM, 1 μM, 10 μM, and 4 mM ATP, respectively. No clear change in slope factor with [ATP] was observed in individual experiments; therefore, the slope factor was shared in the global fit; kT/ez_q = 43 ± 3 mV. (*D*) Q_{tot} as a function of [MgATP]. Continuous lines represent fits using Eq. 1 (n_H = 1) to the whole data set from five patches with $K_{0.5,ATP}$ = 0.43 ± 0.03 μM. To see this figure in color, go online.

Na^+_i (Fig. 6 *A*). The average I_H-V curves from six patches at different [ATP] values (Fig. 6 *B*) demonstrate that the effect of ATP is not saturating at high micromolar concentrations: the average I_H at −140 mV as a function of [ATP] (Fig. 6 *C*) was fitted with the Michaelis-Menten equation (Eq. 1, n_H = 1, *solid line*) with $K_{0.5,ATP}$ = 48 ± 11 μM. This value indicates that high-affinity Na/K pump phosphorylation is insufficient for max I_H, in contrast to the observation of Q_{Na} activation in Fig. 5, and suggests that I_H requires simultaneous low-affinity ATP binding to E2. For comparison, the fit for Q_{tot} (*dotted line* in Fig. 5 *D*, $K_{0.5,ATP}$ = 0.43 ± 0.03 μM) is also shown in Fig. 6 *C*.

To demonstrate the simultaneous requirement of phosphorylation and low-affinity binding, we applied 10 μM ATP, a concentration that would saturate high-affinity phosphorylation (of E1), but not low-affinity binding (to E2), in combination with 1 mM AMPPNP (Fig. 7). A representative experiment from a patch held at −50 mV is shown in Fig. 7 *A* and the average nucleotide-induced I-V curves are shown in Fig. 7 *B*.

Intracellular ion dependence of I_H

Because Na^+_i must be present to phosphorylate the Na/K pump by ATP, we evaluated whether it is possible to activate I_H in the presence of K^+ as the sole intracellular monovalent cation substrate (Fig. 8). MgATP activated I_H in the presence of Na^+_i as well as in the presence of K^+_i, although the ATP-induced current in K^+_i was smaller (Fig. 8, *A* and *B*; $I_{H,K}/I_{H,Na}$ = 0.13 ± 0.01, *n* = 19), in quantitative disagreement with previous reports (17).

In contrast to the results obtained in the presence of Na^+_i, ADP induced the same currents as ATP in the presence of K^+_i (Fig. 8 *B*), suggesting that I_H could be activated without phosphorylation. However, I_H activation by nucleotides in the presence of K^+_i could be due to backdoor phosphorylation

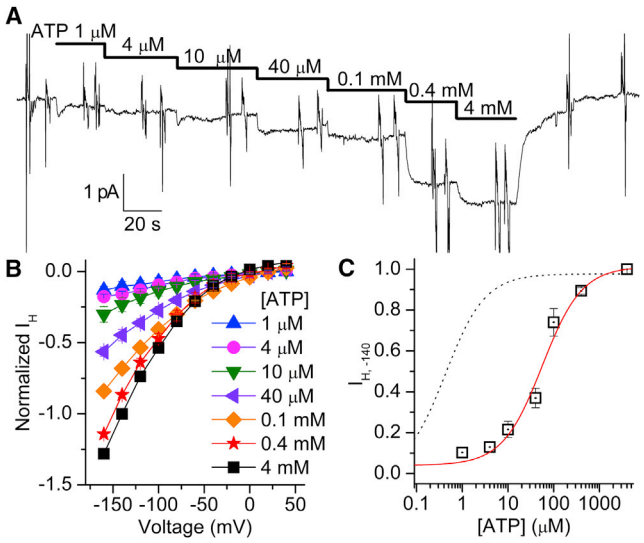

FIGURE 6 ATP activation of I_H. (*A*) Continuous current recording from a patch at V_h = −80 mV, with NMG^+_o (pH 6) in the pipette, to which increasing [ATP] were added in the presence of 20 mM Na^+_i. (*B*) Average I_H-V from six patches at different [ATP], normalized to I_H at −140 mV with 4 mM ATP. (*C*) [ATP] dependence of I_H activation in Na^+_i at −140 mV. The solid line is the fit obtained using a rectangular hyperbola (Eq. 1, n_H = 1) with $K_{0.5ATP}$ = 55.8 μM. The dotted line is the fit from Fig. 5 *D*. To see this figure in color, go online.

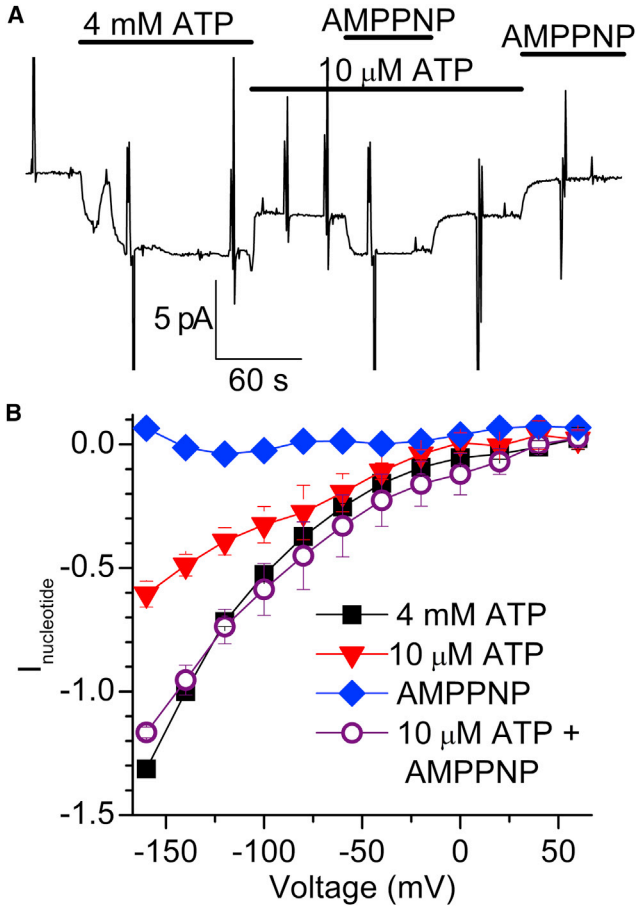

FIGURE 7 I_H in 20 mM Na^+_i requires phosphorylation and ATP binding. (*A*) Recording from a patch at −50 mV on which ATP (10 μM and 4 mM) and AMPPNP (1 mM) were applied as indicated. (*B*) Average current induced by 4 mM ATP, 10 μM ATP, 1 mM AMPPNP, and 10 μM ATP + 1 mM AMPPNP; data from three patches, normalized to I_H at −140 mV in 4 mM MgATP. To see this figure in color, go online.

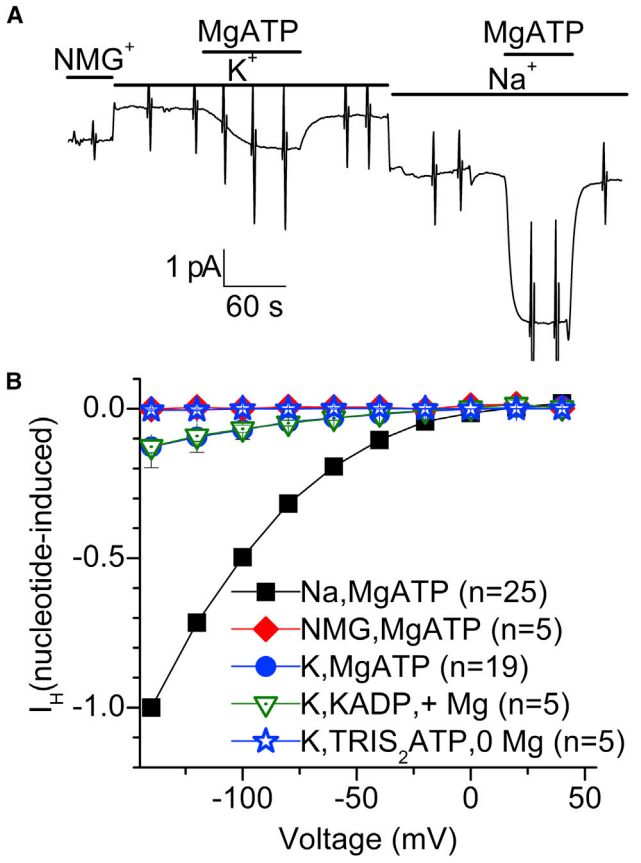

FIGURE 8 I_H with K^+_i. (*A*) Recording from a patch at $V_h = -50$ mV, with NMG^+_o (pH 6) in the pipette, to which 4 mM ATP was added in the presence of Na^+_i or K^+_i. (*B*) I_H-V induced by nucleotides (MgATP, K-ADP, or $TRIS_2$-ATP as indicated) in the presence of 110 mM NMG^+_i, 20 or 110 mM K^+_i, or 20 or 110 mM Na^+_i, normalized to I_H at −140 mV with 4 mM ATP and Na^+_i. The number of experiments is indicated in parentheses. To see this figure in color, go online.

if there is enough free P_i in ATP- and ADP-containing solutions. ATP failed to activate current in the absence of Mg^{2+}_i (Fig. 8 *B*, *open stars*). As Mg^{2+} is essential for phosphorylation, this experiment demonstrates that activation of I_H by MgATP in K^+_i is due to backdoor phosphorylation via the contaminating MgP_i in solution. The free P_i of a 4 mM MgATP solution after 1 h at room temperature was 12 ± 1 μM (measured colorimetrically; see Materials and Methods). To directly demonstrate the effect of P_i, we added 25, 50, and 200 μM P_i to the 20 mM K^+_i + 4 mM MgATP solution (Fig. 9). P_i augmented I_H in a dose-dependent manner, with 200 μM inducing twice as much current as MgATP alone.

Proton current in beryllium-fluoride-inhibited pumps

When bound to the conserved aspartic acid in the P domain of P-type ATPases, beryllium fluoride acts as a phosphate analog forming an NKA-BeF_3^- complex stabilizing an externally-open E2P-like structure (32). Consistent with this, it inhibits Na/K pump cycling by promoting a state capable of binding ouabain with high affinity (33). Recently, utilizing a slightly different *Xenopus*-α1 ouabain-resistant mutant (C113Y), Vedovato and Gadsby (14) showed that injection of beryllium fluoride into *Xenopus* oocytes inhibits NKA function, but does not alter the I_H seen in the absence of Na^+_o and K^+_o. The patch-clamp experiments with NMG^+_o (pH 6) in the pipette (Fig. 10) show that 1) the NKA-BeF_3^- complex transports a slightly larger I_H than 4 mM ATP alone (Fig. 10, *A* and *B*), 2) the effects of beryllium fluoride are irreversible (within the experimental duration; Fig. 10 *B*), and 3) once the E2-BeF_3^- complex is formed, the pump does not require ATP binding to activate I_H (Fig. 10, *A* and *B*).

DISCUSSION

The Post-Albers scheme (34,35) has withstood 50 years of studies and still captures the essence of how the Na/K

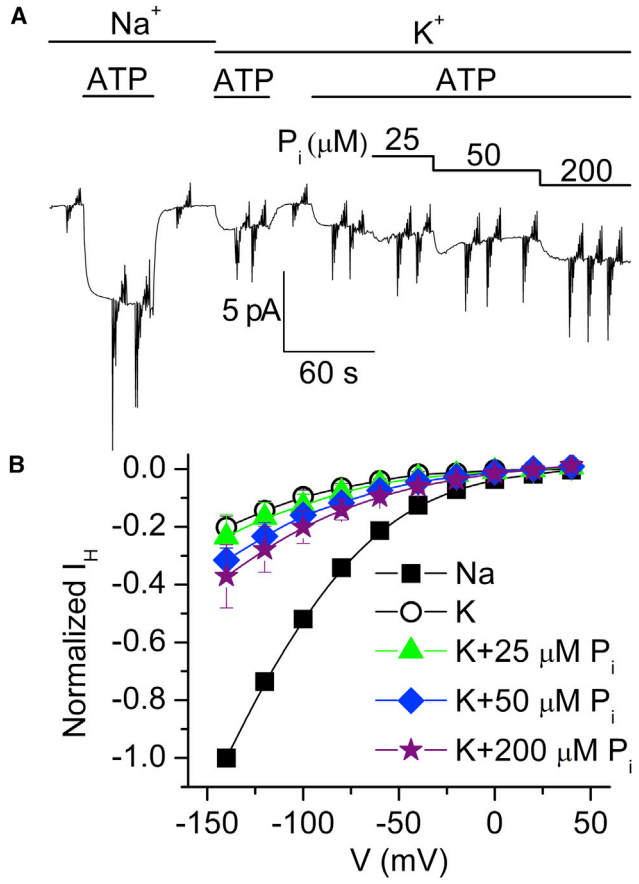

FIGURE 9 Currents activated by P_i in the presence of MgATP. (*A*) Patch recording at −50 mV with NMG^+_o pH 6 in the pipette. I_H was activated by the indicated [P_i] in solution with 20 mM K^+_i and 4 mM ATP. (*B*) I-V plot showing P_i+ATP-activated I_H normalized to I_H activated by 20 mM Na^+_i+ATP at −140 mV ($n = 2$). To see this figure in color, go online.

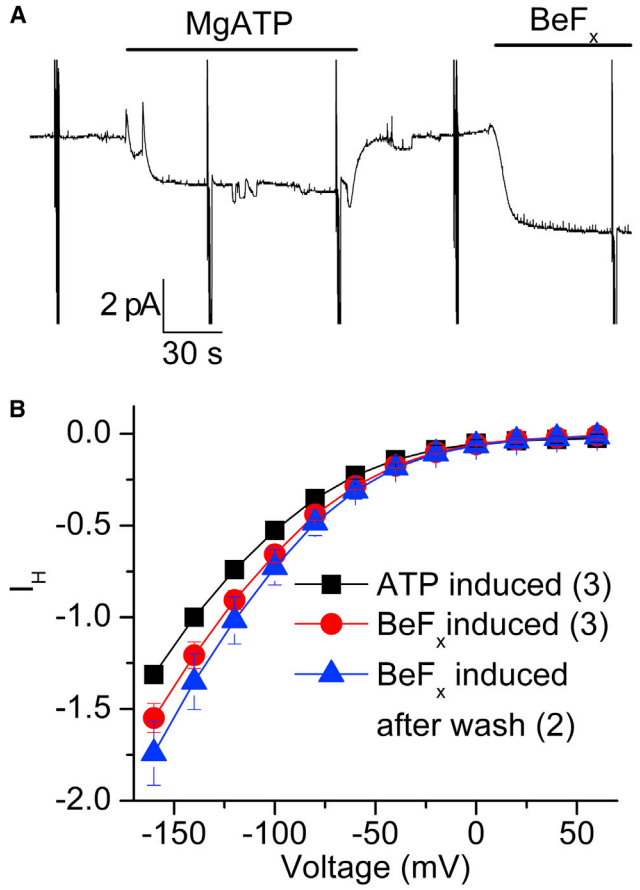

FIGURE 10 Beryllium fluoride activation of I_H. (*A*) Recording from a patch at V_h= −80 mV with NMG^+_o (pH 6) in the pipette, showing activation of inward current by MgATP (4 mM) and by beryllium fluoride (0.5 mM) in the presence of 20 mM Na^+_i. (*B*) Voltage dependence of the average beryllium-fluoride- or ATP-induced current ($n = 3$). The beryllium-fluoride-induced I-V curve was obtained after beryllium fluoride withdrawal ($n = 3$). To see this figure in color, go online.

pump works. Since it was first proposed, many articles have described the equilibrium constants and reaction rates of individual partial reactions using open (e.g., (36)) or sided membrane preparations (e.g., (5,6)). Although in this study we focused on gaining a deeper mechanistic understanding of the inward leak that has been studied by several laboratories in the last few years, the results presented here also shed light on the requirements for the Na^+-dependent transient charge movement that reflects the E2P-E1P transition, on the backdoor phosphorylation of the pump, and on the inhibition of the Na/K pump by beryllium fluoride. Below, we discuss our results in the context of previous studies, beginning with the conditions that facilitate I_H through the Na/K pump.

Conditions needed for I_H when Na^+_i is present

We observed that 4 mM ATP induced a large I_H (Figs. 2, 4, and 8), consistent with all previous whole-cell studies in which I_H was studied with Na^+_i and ATP, including those conducted in oocytes (8–16) and ventricular myocytes (15). If Na^+_i was present without nucleotide, or in the presence of AMPPNP (Fig. 7), ADP (Fig. 8), and AMPPCP (not shown), all of the pumps were trapped in the E1 state with three Na^+ ions bound (Fig. 1) and I_H was absent. The lack of activation by nonhydrolyzable nucleotides demonstrates the requirement for phosphorylation. The high apparent affinity for Na^+_i activation of I_H ($K_{0.5}$ = 1.8 mM; Fig. 3) is consistent with this interpretation.

Although phosphorylation is necessary in the presence of Na^+_i, it is not sufficient to produce maximal I_H. The low affinity seen in the ATP concentration dependence for I_H activation (Fig. 6) indicates that in addition to phosphorylation, maximal I_H also requires nucleotide binding to E2P, a conformation with low affinity for ATP (30,31). The nearly identical currents observed with 4 mM ATP or with 10 μM ATP + 1 mM AMPPNP (Fig. 7) further demonstrate that robust downhill proton import only occurs from E2P when ATP is bound. Thus, binding of ATP to the ion-empty E2P state (reached after release of Na^+ by the phosphorylated

pump) is required to promote a conformational change, which activates I_H. This ATP-induced conformational change, which must not involve a full return to E1 (as it would shut down I_H), probably causes the high temperature dependence previously described for I_H (12). (It is hard to conclude definitely whether the small (10% of maximal) I_H observed in the three experiments with 1 μM ATP (Fig. 6) represents the I_H supported by phosphorylated pumps without ATP bound.)

Activation of I_H without Na^+_i with K^+_i; backdoor phosphorylation

Rettinger (17) utilized patches excised from oocytes (expressing Torpedo α1/β1 and rat α1/mouse β1 Na^+,K^+-ATPase) to partially study the intracellular conditions in which I_H is observed. The author reported that K^+_i and Na^+_i induced nearly identical I_H values in the presence of MgATP. In contrast, we observed a significantly smaller I_H in K^+_i compared with Na^+_i. Given our results demonstrating the requirement of pump phosphorylation with Na^+_i (Fig. 2), it was unexpected to observe I_H in K^+_i, because ATP cannot phosphorylate pumps in the absence of Na^+_i. Even more surprising, though, was the finding that ADP, which can mimic ATP binding at the low-affinity site (30) without ever producing phosphoenzyme (31), also activated I_H.

Therefore, we thought that spontaneous ATP or ADP hydrolysis was supplying enough inorganic phosphate for backdoor phosphorylation of E2(K2)-occluded pumps, thus promoting E2P in a fraction of the pumps. Although we were careful to take out frozen aliquots just before applying them to the patch, it is possible that nucleotide hydrolysis occurred during shipment or after storage (in neutral solution at -20°C). We did determine the level of free P_i with one preparation of fresh MgATP at ~12 μM, but total P_i could vary from batch to batch and with time in the freezer. Because I_H was not activated by ATP without Mg^{2+}, we conclude that formation of the phosphoenzyme is required for I_H. This conclusion is based on the fact that Mg^{2+} is required for backdoor phosphorylation, but not for intracellular K^+ binding or for acceleration of K^+ deocclusion (30).

The $K_{0.5}$ for P_i varies with the experimental conditions, being reduced by K^+ and ATP (37,38) or occluded Rb^+ (39), and in our conditions it is expected to be above 250 μM, consistent with the doubling of I_H by addition of 200 μM P_i (Fig. 9). The lack of I_H when only NMG^+_i is present must mean that in the presence of NMG^+ alone, the pump remains in an E1 state, impairing backdoor phosphorylation. Therefore, in the presence of K^+_i, the pumps bind K^+_i and transition to E2(K2), from where a fraction of them are phosphorylated by MgP_i, releasing K^+ externally. This induces I_H as the pumps remain in E2P with ATP bound.

Q_{Na} and I_H requirements: similarities and distinctions

The dependence of Q_{Na} on MgATP confirms our previous report (24) that this mode of function absolutely requires ATP-dependent phosphorylation in the presence of Na^+_i. It appears that ATP binding does not significantly affect the position of the Q-V curve on the voltage axis, as the $V_{1/2}$ values of the Q-V curves were not significantly different between ATP concentrations, with the possible exception of 0.2 μM (Fig. 5 *C*); the apparent shift in the curve at 0.2 μM is probably due to the small signal size. The lack of an obvious effect of ATP on $V_{1/2}$ (the differences at 0.2 μM ATP were not significant in the ANOVA) contrasts the effects of ADP described by Peluffo (40), probably reflecting that only ADP accelerates dephosphorylation of E1P (2).

Conformation mimicked by beryllium-fluorinated pumps

A novel, to our knowledge, observation is that beryllium fluoride activates I_H maximally, even after ATP has been removed (Fig. 10). This indicates that the E2-BeF_3^--inhibited Na^+,K^+ ATPase mimics an E2P state (or states, as this is not a simple open channel) with ATP bound. Although this is not clear in the SERCA crystal structures in complex with BeF_3^-, which were solved in the presence or absence of nucleotides (41,42), a recent structure of bovine $\alpha1\beta1\gamma$-BeF_3^- showed a 10° difference in the position of the N-domain compared with the pig $\alpha1\beta1\gamma$-BeF_3^- structure complexed with ouabain (43). Because a similar tilt in the N-domain was observed in pig $\alpha1\beta1\gamma$-E2BeF_3^- in complex with bufalin, the authors favored the idea that movement of the N-domain is not induced by the phosphate analog inhibitor, but by the crystal-packing conditions. Our results obtained with a functioning Na/K pump show that BeF_3^- may indeed induce movement of the N-domain to mimic the ATP-bound E2P, which certainly may be enhanced by some experimental or crystallographic conditions.

CONCLUSIONS

Our results demonstrate that the wild-type inward proton current mediated by the Na/K pump occurs whenever a significant number of pumps are open extracellularly in the presence of high intracellular ATP and externally nonsaturating concentrations of Na^+ and K^+. This externally open, phosphorylated state can be achieved by Na/K pump phosphorylation 1) in the presence of intracellular Na^+ and ATP, moving the pump in the forward direction toward E2P, or 2) in the presence of intracellular K^+ and P_i, moving the pump in the reverse direction. Extrapolating from the data of Post and Sen (35) and Heyse et al. (36), it appears

that as little as 15 μM P_i can induce some E2P formation, which could explain the I_H we observed in the presence of K^+_i and Mg^{2+}_i (Fig. 8 *B*) (we estimate that 10–20 μM P_i was present in these experiments due to contamination from the commercial batches of ATP used). It will be interesting to evaluate whether similar mechanisms are involved in NKA mutations associated with familial hemiplegic migraine or hyperaldosteronism, where these pumps may exhibit I_H under physiological conditions.

AUTHOR CONTRIBUTIONS

K.S.S. and D.J.M. performed research and analyzed data. C.G. designed research and wrote the manuscript. P.A. designed and performed research, analyzed data, and wrote the manuscript.

ACKNOWLEDGMENTS

We thank Dr. Luis Reuss for critically reading the manuscript, and Adam Bernal for oocyte preparation.

This work was supported by grants from the National Science Foundation (MCB-1515434 to P.A. and R15-GM061583 to C.G.).

REFERENCES

1. Sen, A. K., and R. L. Post. 1964. Stoichiometry and localization of adenosine triphosphate-dependent sodium and potassium transport in the erythrocyte. *J. Biol. Chem.* 239:345–352.
2. Post, R. L., A. K. Sen, and A. S. Rosenthal. 1965. A phosphorylated intermediate in adenosine triphosphate-dependent sodium and potassium transport across kidney membranes. *J. Biol. Chem.* 240:1437–1445.
3. Rakowski, R. F., D. C. Gadsby, and P. De Weer. 1989. Stoichiometry and voltage dependence of the sodium pump in voltage-clamped, internally dialyzed squid giant axon. *J. Gen. Physiol.* 93:903–941.
4. Nakao, M., and D. C. Gadsby. 1986. Voltage dependence of Na translocation by the Na/K pump. *Nature.* 323:628–630.
5. Holmgren, M., J. Wagg, …, D. C. Gadsby. 2000. Three distinct and sequential steps in the release of sodium ions by the Na+/K+-ATPase. *Nature.* 403:898–901.
6. Castillo, J. P., H. Rui, …, M. Holmgren. 2015. Mechanism of potassium ion uptake by the Na(+)/K(+)-ATPase. *Nat. Commun.* 6:7622.
7. Peluffo, R. D., and J. R. Berlin. 1997. Electrogenic K+ transport by the Na(+)-K+ pump in rat cardiac ventricular myocytes. *J. Physiol.* 501:33–40.
8. Rakowski, R. F., L. A. Vasilets, …, W. Schwarz. 1991. A negative slope in the current-voltage relationship of the Na+/K+ pump in Xenopus oocytes produced by reduction of external [K+]. *J. Membr. Biol.* 121:177–187.
9. Efthymiadis, A., J. Rettinger, and W. Schwarz. 1993. Inward-directed current generated by the Na+,K+ pump in Na(+)- and K(+)-free medium. *Cell Biol. Int.* 17:1107–1116.
10. Li, C., K. Geering, and J. D. Horisberger. 2006. The third sodium binding site of Na,K-ATPase is functionally linked to acidic pH-activated inward current. *J. Membr. Biol.* 213:1–9.
11. Wang, X., and J. D. Horisberger. 1995. A conformation of Na(+)-K+ pump is permeable to proton. *Am. J. Physiol.* 268:C590–C595.
12. Meier, S., N. N. Tavraz, …, T. Friedrich. 2010. Hyperpolarization-activated inward leakage currents caused by deletion or mutation of carboxy-terminal tyrosines of the Na+/K+-ATPase alpha subunit. *J. Gen. Physiol.* 135:115–134.
13. Poulsen, H., H. Khandelia, …, P. Nissen. 2010. Neurological disease mutations compromise a C-terminal ion pathway in the Na+/K+-ATPase. *Nature.* 467:99–102.
14. Vedovato, N., and D. C. Gadsby. 2014. Route, mechanism, and implications of proton import during Na+/K+ exchange by native Na+/K+-ATPase pumps. *J. Gen. Physiol.* 143:449–464.
15. Mitchell, T. J., C. Zugarramurdi, …, P. Artigas. 2014. Sodium and proton effects on inward proton transport through Na/K pumps. *Biophys. J.* 106:2555–2565.
16. Ratheal, I. M., G. K. Virgin, …, P. Artigas. 2010. Selectivity of externally facing ion-binding sites in the Na/K pump to alkali metals and organic cations. *Proc. Natl. Acad. Sci. USA.* 107:18718–18723.
17. Rettinger, J. 1996. Characteristics of Na+/K(+)-ATPase mediated proton current in Na+- and K+-free extracellular solutions. Indications for kinetic similarities between H+/K(+)-ATPase and Na+/K(+)-ATPase. *Biochim. Biophys. Acta.* 1282:207–215.
18. Azizan, E. A., H. Poulsen, …, M. J. Brown. 2013. Somatic mutations in ATP1A1 and CACNA1D underlie a common subtype of adrenal hypertension. *Nat. Genet.* 45:1055–1060.
19. Tavraz, N. N., T. Friedrich, …, M. Dichgans. 2008. Diverse functional consequences of mutations in the Na+/K+-ATPase alpha2-subunit causing familial hemiplegic migraine type 2. *J. Biol. Chem.* 283:31097–31106.
20. Friedrich, T., N. N. Tavraz, and C. Junghans. 2016. ATP1A2 mutations in migraine: seeing through the facets of an ion pump onto the neurobiology of disease. *Front. Physiol.* 7:239.
21. Price, E. M., and J. B. Lingrel. 1988. Structure-function relationships in the Na,K-ATPase alpha subunit: site-directed mutagenesis of glutamine-111 to arginine and asparagine-122 to aspartic acid generates a ouabain-resistant enzyme. *Biochemistry.* 27:8400–8408.
22. Gatto, C., S. Lutsenko, and J. H. Kaplan. 1997. Chemical modification with dihydro-4,4′-diisothiocyanostilbene-2,2′-disulfonate reveals the distance between K480 and K501 in the ATP-binding domain of the Na,K-ATPase. *Arch. Biochem. Biophys.* 340:90–100.
23. Johnson, N. A., F. Liu, …, C. Gatto. 2009. A tomato ER-type Ca2+-ATPase, LCA1, has a low thapsigargin-sensitivity and can transport manganese. *Arch. Biochem. Biophys.* 481:157–168.
24. Yaragatupalli, S., J. F. Olivera, …, P. Artigas. 2009. Altered Na+ transport after an intracellular alpha-subunit deletion reveals strict external sequential release of Na+ from the Na/K pump. *Proc. Natl. Acad. Sci. USA.* 106:15507–15512.
25. Patti, M., C. Fenollar-Ferrer, …, I. C. Forster. 2016. Cation interactions and membrane potential induce conformational changes in NaPi-IIb. *Biophys. J.* 111:973–988.
26. Hilgemann, D. W. 1994. Channel-like function of the Na,K pump probed at microsecond resolution in giant membrane patches. *Science.* 263:1429–1432.
27. Blanco, G. 2005. The NA/K-ATPase and its isozymes: what we have learned using the baculovirus expression system. *Front. Biosci.* 10:2397–2411.
28. Vilsen, B. 1993. A Glu329–>Gln variant of the alpha-subunit of the rat kidney Na+,K+-ATPase can sustain active transport of Na+ and K+ and Na+,K+-activated ATP hydrolysis with normal turnover number. *FEBS Lett.* 333:44–50.
29. Artigas, P., and D. C. Gadsby. 2004. Large diameter of palytoxin-induced Na/K pump channels and modulation of palytoxin interaction by Na/K pump ligands. *J. Gen. Physiol.* 123:357–376.
30. Forbush, B., 3rd 1987. Rapid release of 42K and 86Rb from an occluded state of the Na,K-pump in the presence of ATP or ADP. *J. Biol. Chem.* 262:11104–11115.
31. Post, R. L., C. Hegyvary, and S. Kume. 1972. Activation by adenosine triphosphate in the phosphorylation kinetics of sodium and potassium ion transport adenosine triphosphatase. *J. Biol. Chem.* 247:6530–6540.

32. Olesen, C., M. Picard, …, P. Nissen. 2007. The structural basis of calcium transport by the calcium pump. *Nature.* 450:1036–1042.

33. Cornelius, F., Y. A. Mahmmoud, and C. Toyoshima. 2011. Metal fluoride complexes of Na,K-ATPase: characterization of fluoride-stabilized phosphoenzyme analogues and their interaction with cardiotonic steroids. *J. Biol. Chem.* 286:29882–29892.

34. Albers, R. W. 1967. Biochemical aspects of active transport. *Annu. Rev. Biochem.* 36:727–756.

35. Post, R. L., and A. K. Sen. 1965. An enzymatic mechanism of active sodium and potassium transport. *J. Histochem. Cytochem.* 13:105–112.

36. Heyse, S., I. Wuddel, …, W. Stürmer. 1994. Partial reactions of the Na,K-ATPase: determination of rate constants. *J. Gen. Physiol.* 104: 197–240.

37. Askari, A., and W. H. Huang. 1984. Reaction of (Na+ + K+)-dependent adenosine triphosphatase with inorganic phosphate. Regulation by Na+, K+, and nucleotides. *J. Biol. Chem.* 259:4169–4176.

38. Huang, W. H., and A. Askari. 1984. Regulation of (Na++K+)-ATPase by inorganic phosphate: pH dependence and physiological implications. *Biochem. Biophys. Res. Commun.* 123:438–443.

39. Forbush, B., 3rd 1987. Rapid release of 42K or 86Rb from two distinct transport sites on the Na,K-pump in the presence of Pi or vanadate. *J. Biol. Chem.* 262:11116–11127.

40. Peluffo, R. D. 2004. Effect of ADP on Na+-Na+ exchange reaction kinetics of Na,K-ATPase. *Biophys. J.* 87:883–898.

41. Toyoshima, C., S. Yonekura, …, S. Iwasawa. 2011. Trinitrophenyl derivatives bind differently from parent adenine nucleotides to Ca2+-ATPase in the absence of Ca2+. *Proc. Natl. Acad. Sci. USA.* 108:1833–1838.

42. Clausen, J. D., M. Bublitz, …, P. Nissen. 2016. Crystal structure of the vanadate-inhibited Ca2+-ATPase. *Structure.* 24:617–623.

43. Gregersen, J. L., D. Mattle, …, L. Reinhard. 2016. Isolation, crystallization and crystal structure determination of bovine kidney Na+,K+-ATPase. *Acta Crystallogr. F Struct. Biol. Commun.* 72:282–287.